J. Electrochem. Sci. Eng. **12(1)** (2022) 185-197; http://dx.doi.org/10.5599/jese.1211

Open Access : : ISSN 1847-9286

https://pub.iapchem.org/ojs/index.php/JESE

Original scientific paper

Electrochemical sensor based on MWCNTs/Co_3O_4/SPGE for simultaneous detection of Sudan I and Bisphenol A

Afsaneh Hajializadeh✉

Department of Natural Resources, Sirjan Branch, Islamic Azad University, Sirjan, Iran

Corresponding author: ✉hajalizadeh.813@gmail.com

Received: December 13, 2021; Accepted: December19, 2021; Published: February 9, 2022

Abstract

This paper presents a sensitive simultaneous detection procedure for Sudan I and bisphenol A based on the multiwalled carbon nanotubes (MWCNTs)/Co_3O_4 nanocomposite modified screen-printed graphite electrode (SPGE). This MWCNTs/Co_3O_4 nanocomposite was prepared by the hydrothermal technique, and characterized by Fourier transform infrared (FT-IR) spectroscopy, field emission scanning electron microscopy (FE-SEM) and X-ray diffraction (XRD). The electrochemical properties of MWCNTs/Co_3O_4 nanocomposite modified SPGE were analyzed by cyclic voltammetry (CV), differential pulse voltammetry (DPV), chronoamperometry (CHA), as well as linear sweep voltammetry (LSV). From the electrochemical results, a synergy between MWCNTs and Co_3O_4 nanoparticles (NPs) was detected as improved interfacial electron transfer, which was accompanied by a greater catalytic function for electrochemical oxidation of Sudan I. Based on the optimized condition, MWCNTs/Co_3O_4/SPGE exhibited the linear dynamic ranging between 0.05 and 600.0 µM detection of Sudan I with a limit of detection (LOD) 0.02 µM. Also, the as-prepared electrode was assessed for simultaneous detection of Sudan I and Bisphenol A. In the course of electrooxidation processes of these analytes, two complete peaks at 380 and 520 mV were observed on the modified electrode. At the end, utility of this new electrochemical sensor was performed to determine Sudan I and Bisphenol A in some real samples with good accuracy and precision.

Keywords

Electroanalysis; voltammetry; azo dyes; food analysis; modified electrodes; SPGE; MWCNTs/Co_3O_4

Introduction

Sudan I (1-phenylazo-2-naphtol) is a synthetic azo dye commonly employed as one of the coloring materials in industrial products like shoes, textile, oil, plastic, printing ink, cosmetics, as well as floor polish [1]. Moreover, Sudan I is also proposed as food additive material, sauces, chili powder, readymade meals, and chutneys because of its bright red colour, affordability, and coloring fastness.

However, in the case of ingestion of the materials consisting of Sudan I by human bodies, carcinogenic amines would be produced following the metabolism process [2]. Hence, European Union (EU) and Food Standards Agency have strongly forbidden the utilization of Sudan I as an additive in foodstuff because of its higher teratogenetic and carcinogenic nature. Despite the legal prohibitions, Sudan I circulates in the food markets due to temptations for massive profits [3]. Thus, the determination of Sudan I residues in the food products would be necessary to preclude health risks to humans.

Experts in the field have introduced Bisphenol A (4,4‘-(propane-2,2-diyl)diphenol) (BPA) as one of the key monomeric compounds applied in fabricating polycarbonate and epoxy in plastic outputs. They have also been employed for making diverse plastic products like water and milk bottles, food containers, bottles for infant feeding, dental fillings, bottle tops, table-ware, food cans, and other storage vessels [4-6]. Moreover, BPA can migrate from plastic products into the environment and food chain resulting in considerable humans' exposure [7]. Additionally, BPA has been proposed as one of the endocrine-disrupting compounds associated with several sorts of health issues like cancer progression and reproduction issues [8,9]. Considering public health, it would be of high significance to develop a valid analytical procedure to determine BPA.

Several analytical methods such as gas chromatography-mass spectrometry (GC–MS) [10], high-performance liquid chromatography (HPLC) [11,12], fluorescence [13], capillary electrophoresis [14], surface-enhanced Raman scattering spectroscopy [15], and chemiluminescence [16,17] have been developed for detecting Bisphenol A and Sudan I. These techniques showed good outputs, although, they might be laborious and demand numerous raw materials, professional workforce, and costly instruments.

In this regard, researchers have also studied electrochemical sensing as one of the very attractive fields in analytical chemistry [18-22]. Electrochemical methods are broadly employed for the analysis of biological, environmental, food, pharmaceutical and industrial compounds due to merits such as fast responses, higher sensitivity, lower costs, portability, and ease of operation [23-29].

It is notable that as an electrochemical sensing platform, the screen-printed electrode (SPE) has been largely attracted because of merits like easier application, portability, and affordability [30,31]. Hence, the screen-printed technology significantly contributes to the transition from the conventional unwieldy electrochemical cells to the portable miniaturized electrodes, satisfying the on-site analysis requirements [32,33].

In the electrochemical approach, using a proper electrode is of utmost importance. In this regard, developing the modified substances for improving the electrochemical response of the electrodes would be a challenging task [34-40]. In recent years, researchers have focused on the designing and synthesizing nanomaterials for various applications due to their unique physical and chemical properties [41-43]. Investigations demonstrated that electrodes modified by catalytically active nanomaterials might enhance efficient mass transfer, achieve more acceptable control, and enhance the active specific surface area in a local micro-environment, improving the sensitivity and selectivity of electrochemical sensors [44-49].

Experts in the field have largely employed the carbon nanotubes (CNTs) in the fabrication of electrochemical sensors because of the respective merits like higher carrier mobility, a larger surface-to-volume ratio, good conductivity, and flexibility. CNTs are specific carbon materials with cylindrical curled graphitic sheets [50]. Numerous investigations have shown that constructing the hybrid catalysts *via* immobilization of metal and metal oxide nanoparticles (NPs) on carbon nanotubes can improve their electrochemical responses [51,52]. Furthermore, nanostructured transition metal

oxides contribute significantly to the improvement of sensitivity and stability of sensors. It should be mentioned that among the family of transition metal oxides, nanostructures of cobalt oxide (Co_3O_4) exhibited specific electrocatalytic activity for detecting different compounds [53-55]. The possible cause would be higher activity and selectivity of the metal oxide catalysts resulting from the differences in oxygen defects, oxygen absorbed in various states of cobalt in Co_3O_4 (a mixed valance state of Co(II) and Co(III)), as well as oxygen holes [56].

In the present report, MWCNTs/Co_3O_4 nanocomposite was prepared and employed for the modification of SPGE. The modified SPGE was then utilized to simultaneously detect Sudan I and Bisphenol A.

Experimental

Chemicals and instrumentations

According to the research design, each chemical was of the analytical reagent grade without additional purification. $Co(CH_3CO_2)_2$ $4H_2O$, sodium hydroxide, ethanol, $NH_3{\cdot}H_2O$ (25 to 28 wt.%), and MWCNTs-COOH (purity >95 %) were supplied from Aldrich. Sudan I, Bisphenol A and other chemicals were supplied from the Merck Company (Darmstadt, Germany). Phosphate buffer solutions (PBS) were prepared from H_3PO_4 and the respective salts (KH_2PO_4, K_2HPO_4 and K_3PO_4) (Merck). Food samples such as ketchup sauce, tomato paste and chili powder were purchased from a local store in Kerman, Iran. Nano-pure (18 MΩ·cm) water from a Milli-pore MilliQ system (Bedford) was applied to prepare all solutions.

Electrochemical experiments were recorded using an Auto-lab potentiostat/galvanostat (PGSTAT-302N, Eco Chemie, The Netherlands). Electrochemical tests were carried out using SPGE (DropSens, DRP-110, Spain). Electrochemical cells consisted of a three-electrode arrangement with graphite as a counter electrode and graphite in 4 mm diameter as a working electrode. In addition, a silver pseudo-reference electrode was used to complete the circuit. pH values were measured using a digital pH meter (Metrohm 710).

Fourier transform infrared (FT-IR) spectra of the synthesized nanocomposite were recorded using a spectrometer (SHIMADZU Corporation, Kyoto, Japan) between 4000 and 400 cm^{-1}, applying KBr pellets. XRD patterns were examined with the XRD device model X'Pert Pro, the Netherlands, while EDX and FE-SEM images were obtained using MIRA3TESCAN-XMU.

Synthesis of the MWCNTs/Co_3O_4 nanocomposite

A hydrothermal approach was used for preparing MWCNTs decorated with Co_3O_4 NPs. Firstly, 20 mg of MWCNTs-COOH were dispersed into 12.5 mL of ethanol, and 0.25 g $Co(CH_3CO_2)_2{\cdot}4H_2O$ was added to the mixture for sonication during 40 min. Then, 2.5 mL of aqueous NH_3 were dropped into the solution and vigorously stirred. The homogeneous slurry was taken to a Teflon-lined stainless steel autoclave, sealed, and heated at 150 °C for 3 h. After cooling the solution to the room temperature, water and ethanol were used to wash the products and achieved MWCNTs/Co_3O_4 nanocomposite followed by the drying process at 60 °C for 8 hours.

Modification of SPGE

The construction of MWCNTs/Co_3O_4 nanocomposite over the SPGE surface was accomplished in this way: 1 mg of MWCNTs/Co_3O_4 nanocomposite was suspended in 1 mL of the distilled water for forming the suspension, which was sonicated for 20 min to disperse the nanocomposite. Finally, 5 µL aliquot of the suspension was pipetted over the surface of an SPGE and dried at the ambient temperature.

The surface areas of MWCNTs/Co_3O_4/SPGE and bare SPE were obtained by CV using 1 mM $K_3Fe(CN)_6$ at different scan rates. Using Randles-Ševčik formula for MWCNTs/Co_3O_4/SPGE, the electrode surface was determined to be 0.08 cm^2, about 2.5 times greater than bare SPGE.

Preparation of real samples

In this step, 20 mL ethanol were used for mixing ketchup sauce, tomato paste, as well as chili powder, and the obtained mixtures were filtrated after 20 min of ultra-sonication, with 100 mL volumetric flasks employed for collecting the liquid phase. Then, treatment was performed for three times and ethanol was applied for diluting the filtrated sample to the intended volumes.

The tap water gathered from the laboratory was analyzed in twelve hours. Before the analysis process, 0.22 µM cellulose acetate membrane was used to filter the water.

Results and discussion

Characterization of MWCNTs/Co_3O_4 nanocomposite

The FTIR spectrum of MWCNTs/Co_3O_4 nanocomposite is shown in Figure 1. For MWCNTs/Co_3O_4 nanocomposite, two sharp bands are found at 660 and 562 cm^{-1}, indicating presence of Co^{2+} and Co^{3+} in the spinal Co-O stretching vibration, wherein Co^{2+} is associated with the tetrahedral coordinate and Co^{3+} to the octahedral coordinate. The spectra bands at 2921 cm^{-1} to 2854 cm^{-1} are attributed to the asymmetric or symmetric stretching vibrations of C-H in CH_2 and $–CH_3$ group in MWCNTs. The peak at 1641 cm^{-1} (aromatic C=C) can be ascribed to the stretching vibration C=C of sp^2 hypridization in CNT back-bone. The band at ~3442 cm^{-1} is attributed to O–H stretching vibration. FT-IR spectrum confirmed the decoration of MWCNTs with Co_3O_4 nanoparticles.

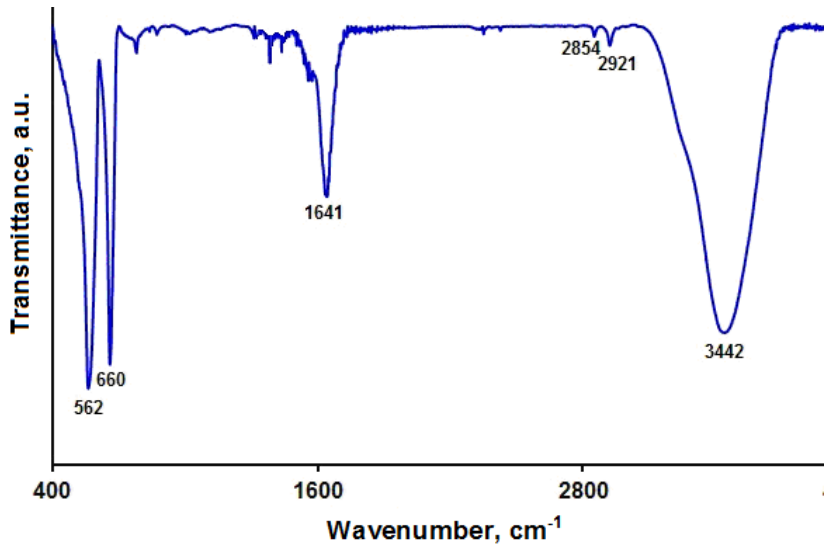

Figure 1. *FT-IR spectrum of MWCNTs/Co_3O_4 nanocomposite*

The crystal structure of MWCNTs/Co_3O_4 nanocomposite was identified by XRD. The XRD peaks of the treated MWCNTs/Co_3O_4 and MWCNTs are shown in Figure 2. As can be seen, MWCNTs patterns have two key diffraction peaks at 2θ=25.9° and 43.1°, which belong to the (002) and (100) planes of graphite. Diffraction peaks at 2 θ values of 19.08, 31.3, 36.9, 38.6, 44.9, 55.7, 59.4 and 65.3°° observed for MWCNT/Co_3O_4 nanocomposite correspond to several planes (111) (220) (311) (222) (400) (422) (511) as well as (440) of Co_3O_4. These characteristic peaks belong to the cubic phase of Co_3O_4 (JCPDS, PDF, File No. 00-042-1467). Furthermore, the peaks have higher intensity reflecting acceptable crystallinity of the samples. However, we did not find any impurity, representing the

substantial contribution of the MWCNT/Co_3O_4 nanocomposite. Finally, Debye-Sheerer equation was used for calculating crystallite size (D) of Co_3O_4 NPs:

$$D = K\lambda / \beta \cos \theta \quad (1)$$

Here, λ represents the wavelength, β the peak width at half maximum, and θ diffraction angle. Dimension of Co_3O_4 nanoparticles is found to 23.8 nm.

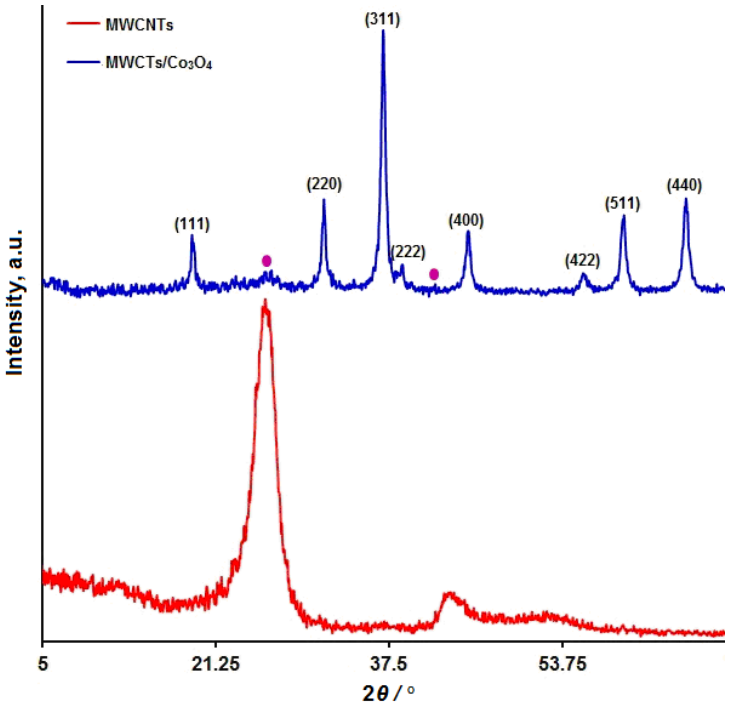

Figure 2. *XRD patterns of MWCNTs and MWCNTs/Co_3O_4 nanocomposite*

Morphology of MWCNTs/Co_3O_4 nanocomposite was investigated using FE-SEM. Figure 3 shows the FE-SEM image of MWCNTs/Co_3O_4 nanocomposite, where the presence of Co_3O_4 nanoparticles coated on the surface of MWCNTs could be evidenced.

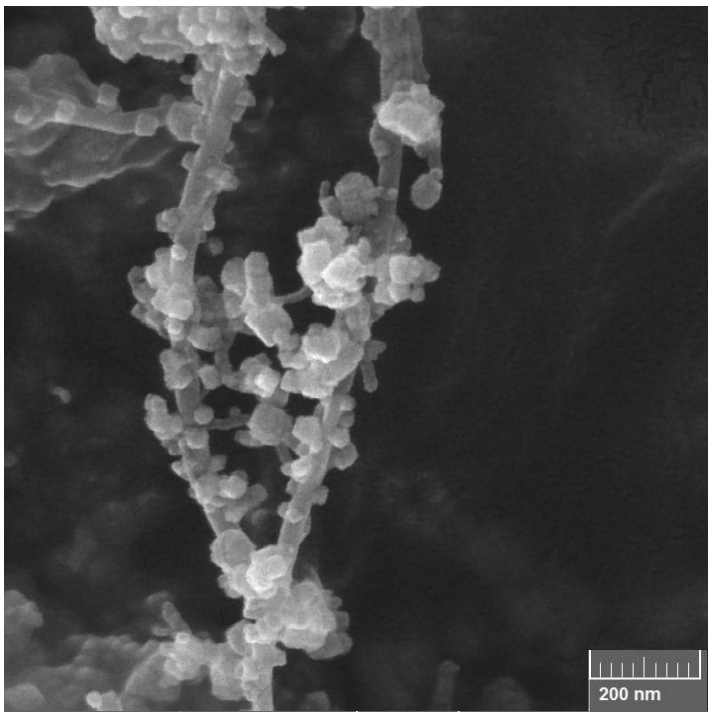

Figure 3. *FE-SEM image of MWCNTs/Co_3O_4 nanocomposite*

Electrocatalytic oxidation of Sudan I at MWCNTs/Co_3O_4/SPGE

For ensuring the best response of MWCNTs/Co_3O_4/SPGE in detecting Sudan I, the influence of the solution pH on the reaction was evaluated by recording voltammetric behavior of MWCNTs/Co_3O_4/SPGE toward 100.0 µM of Sudan I in pH range between 2.0 and 9.0 at the scan rate 50 mV/s. It is shown in Figure 4 that the maximum oxidation current of Sudan I was obtained at pH 7.0. Hence, pH 7.0 was chosen for all further measurements in 0.1 M PBS.

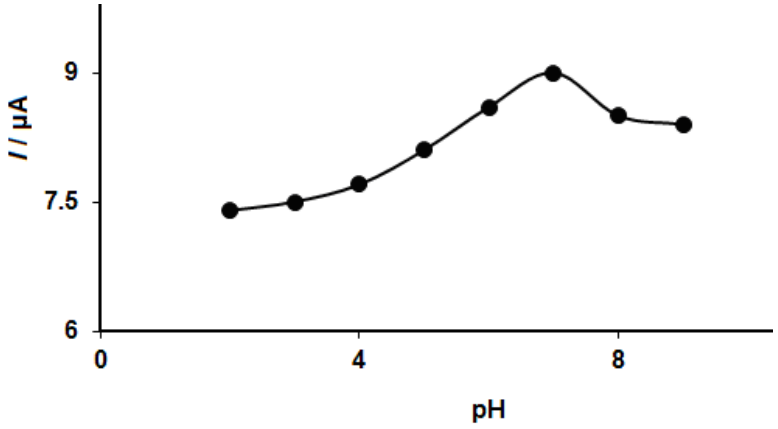

Figure 4. *Plot of I_p vs. pH obtained from DPVs of MWCNTs/Co_3O_4/SPGE in a solution containing 100.0 µM of Sudan I in 0.1 M PBS of different pH (2.0, 3.0, 4.0, 5.0, 6.0, 7.0, 8.0 and 9.0)*

In the next step, the potential application of MWCNTs/Co_3O_4/SPGE for electrooxidation and determination of Sudan I was examined by cyclic voltammetry (CV). Figure 5 depicts the CV response of oxidation of 200.0 µM of Sudan I on (a) bare SPGE, and (b) MWCNTs/Co_3O_4/SPGE in 0.1 M PBS, pH=7.0 at the scan rate 50 mVs^{-1}. As seen in Figure 5, oxidation potential decreased and the peak current height increased for electroxidation of Sudan I at MWCNTs/Co_3O_4/SPGE as compared to bare SPGE. These are probably caused by increasing the rate of the electron transfer process at the modified SPGE electrode, due to the higher surface area, better conductivity of MWCNTs, and electrocatalytic activity of Co_3O_4 nanoparticles.

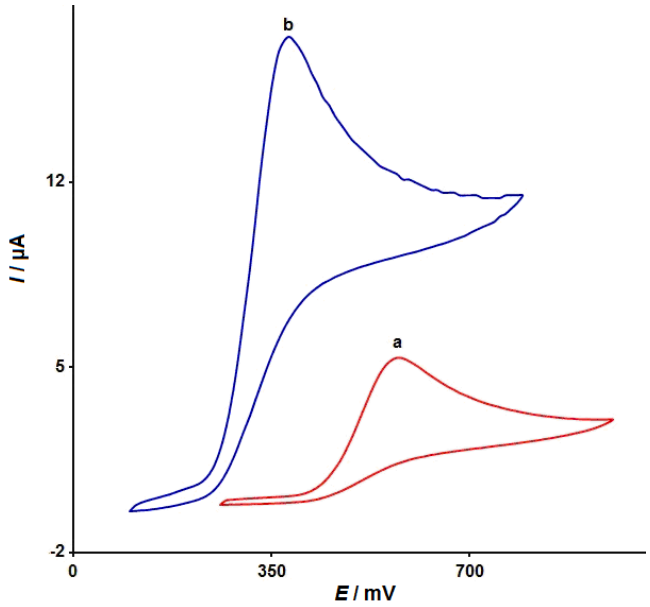

Figure 5. *CV response of 200.0 µM Sudan I in 0.1 M PBS of pH 7.0 at (a) bare SPGE and (b) MWCNTs/Co_3O_4/SPGE*

Effect of potential scan rate on electrochemical response of Sudan I at MWCNTs/Co_3O_4/SPGE

For obtaining information on the kinetics of electrode reactions, the linear sweep voltammetry (LSV) at several scan rates from 10 to 400 mV s^{-1} in 0.1 M PBS, pH 7.0 was applied, and the results

are illustrated in Figure 6. At higher scan rates, a gradual increase of the oxidation peak current can be observed. Obtained voltammograms are irreversible, as were already seen in CV responses shown in Figure 5. Also, Figure 6 shows that the oxidation peak potential is shifted slightly towards positive potentials with increase of the scan rate. According to the linear plot of the oxidation peak current *versus* the square root of the scan rate, shown in the inset of Figure 6, the linear regression eqation was derived. This result indicates that the oxidation process of Sudan I at MWCNTs/Co_3O_4/SPGE electrode is under diffusion control.

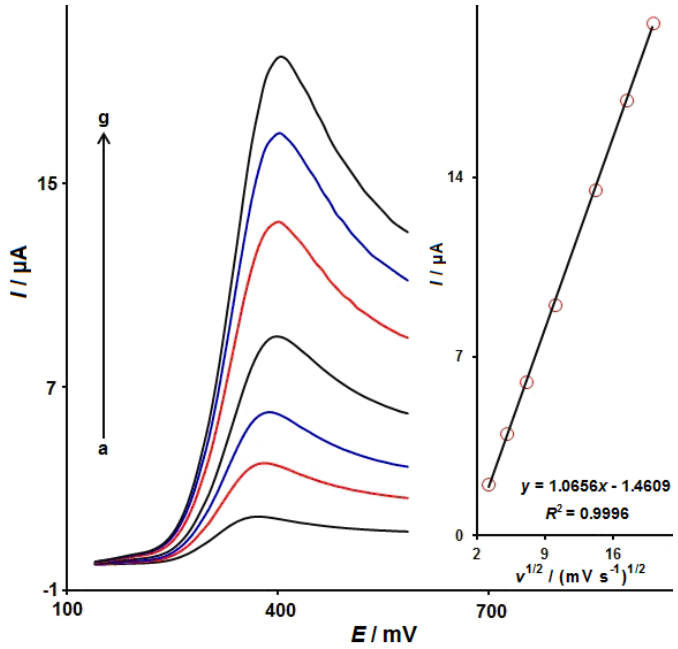

Figure 6. *LSV curves of 50.0 µM of Sudan I in 0.1 M PBS, pH 7.0, at MWCNTs/Co_3O_4/SPGE and different scan rates (a-g refer to 10, 25, 50, 100, 200, 300, and 400 mV s^{-1}). Inset: plot of the oxidation peak current vs. square root of the scan rate*

To define the electron transfer coefficient (α) between Sudan I and MWCNTs/Co_3O_4/SPGE electrode, Tafel diagram (*E vs*. log *I*) was drawn in the inset of Figure 7, using data of the ascending section of the voltammogram registered at 10 mVs^{-1} for 50.0 µM of Sudan I (Figure 7). The calculated slope from the linear plot was equal to 0.084 V^{-1}. From the slope, α value was estimated to 0.3.

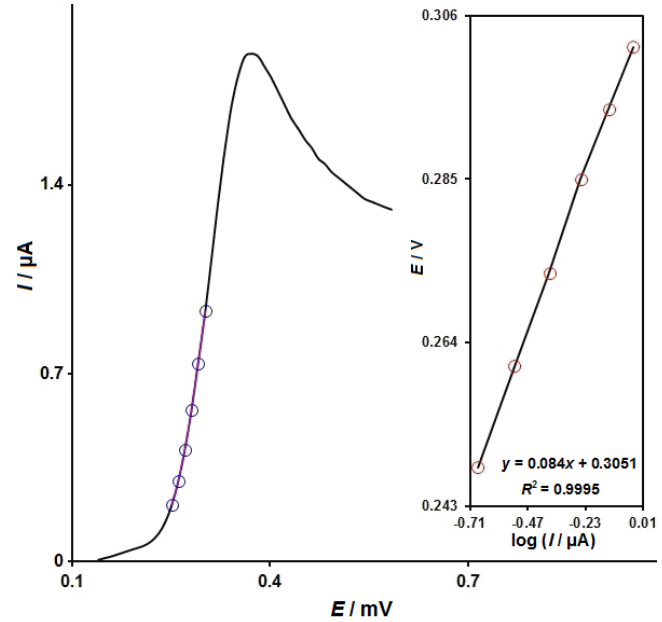

Figure 7. *LSV response (10 mVs^{-1}) of 50.0 µM of sudan I in 0.1 M PBS, pH 7.0 at MWCNTs/Co_3O_4/SPGE. Inset: Tafel plot derived from data of the rising part of voltammogram*

CHA Studies

To measure the diffusion coefficient of Sudan I, chronoamperometry was performed by applying the potential step from 0.0 to 0.43 V.. Figure 8 shows the single-step chronoamperograms recorded for MWCNTs/Co_3O_4/SPGE in the presence of several concentrations of Sudan I. As expected, when Sudan I concentration is increased, the anodic current also increase**s**. The experimental plots of current vs. $t^{-1/2}$ for different concentrations of Sudan I are shown in Figure 8A. The slopes of the straight lines versus the concentration of Sudan I is shown in Figure 8B. Diffusion coefficient was calculated from the slope of the straight line and it equals to 2.0×10^{-5} cm^2 s^{-1}.

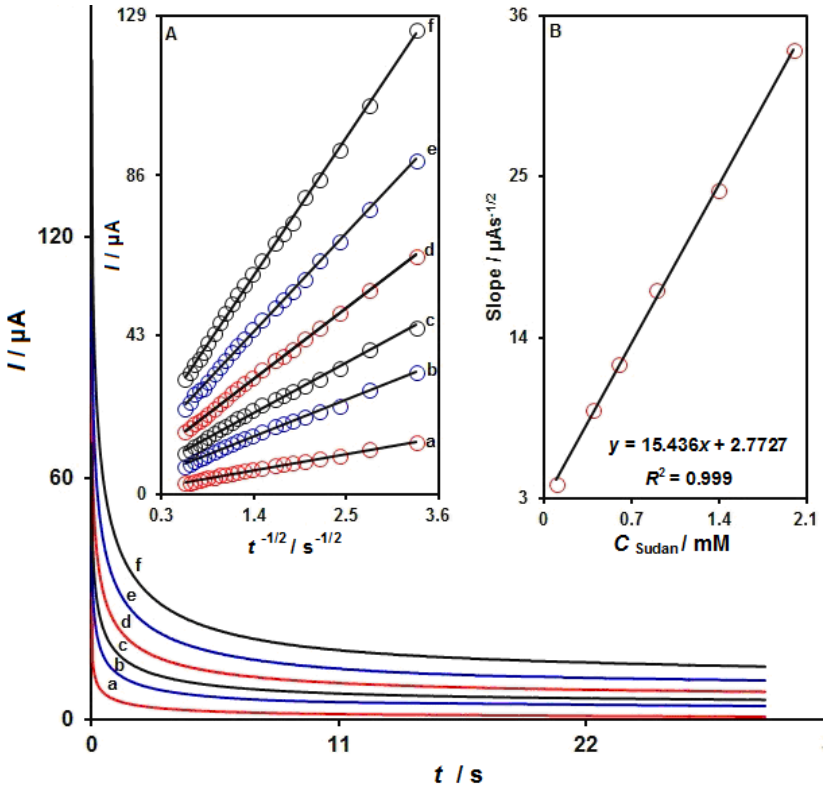

Figure 8. *Chronoamperograms obtained* for *MWCNTs/Co_3O_4/SPGE in 0.1 M PBS, pH 7.0* at *different concentrations of Sudan I (a–f relate to 0.1, 0.4, 0.6, 0.9, 1.4 and 2.0 mM). Inset A: plot of I vs. $t^{-1/2}$ obtained from chronoamperograms a to f. Inset B: plot of straight line slope vs. concentration of Sudan I.*

Detection of Sudan I at MWCNTs/Co_3O_4/SPGE by DPV technique

Differential pulse voltammetry (DPV) technique was employed for determining Sudan I concentration due to its higher sensitivity as well as accuracy leading to lower limit of detection (LOD) values. Figure 9 represents differential pulse voltammograms observed at different concentrations of Sudan I in 0.1 M PBS, pH 7.0 (step potential = 0.01 V and pulse amplitude = 0.025 V). Obviously, oxidation peak current increased with the increase of Sudan I concentration and the inset of Figure 9 demonstrates the linearity of current peak height and concentration of Sudan I. The linear regression has an equation I_{pa} = 0.0817 $C_{sudan\ I}$ + 1.1311 (R^2 = 0.9997). The sensitivity of MWCNTs/Co_3O_4/SPGE is 0.0817 µA μM^{-1}.

The detection limit, C_m, of Sudan I was obtained using the equation (2):

$$C_m = 3s_b / m \quad (2)$$

In the above equation, m is the slope of the calibration plot (0.817 µA μM^{-1}) and s_b is the standard deviation of the blank response obtained from 20 replicate measurements of the blank solution. The detection limit of Sudan I was calculated as 0.02 µM.

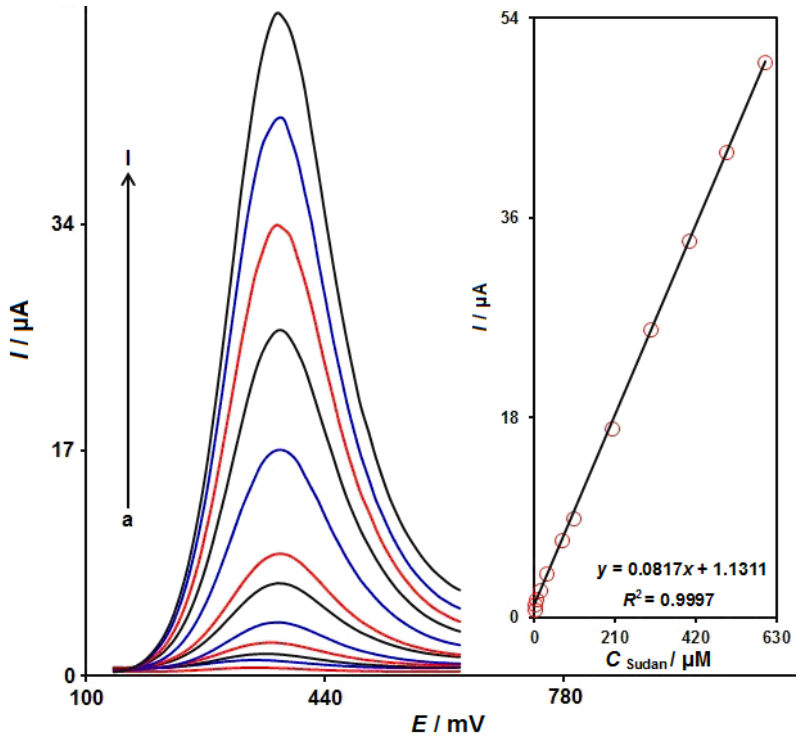

Figure 9. *DPV responses of* different concentrations of *Sudan I at MWCNTs/Co_3O_4/SPGE in 0.1 M PBS, pH 7.0 (a-l refer to 0.05, 0.5, 5.0, 15.0, 30.0, 70.0, 100.0, 200.0, 300.0, 400.0, 500.0 and 600.0 µM). Inset: calibration curve of DPV peak* current *against concentration of Sudan I*

Simultaneous detection of Sudan I and Bisphenol A at MWCNTs/Co_3O_4/SPGE

A simultaneous test of Sudan I and Bisphenol A was carried out by DPV (step potential = 0.01 V and pulse amplitude = 0.025 V) in 0.1 M PBS, pH 7.0. In Fig. 10, two distinctive oxidation peaks of Sudan I and Bisphenol A could be discerned. The peak currents increased linearly with the increase of analyte concentrations without any interference (Figures 10A and 10B). Therefore, a possible simultaneous assay of Sudan I and Bisphenol A could be made with MWCNTs/Co_3O_4/SPGE sensor.

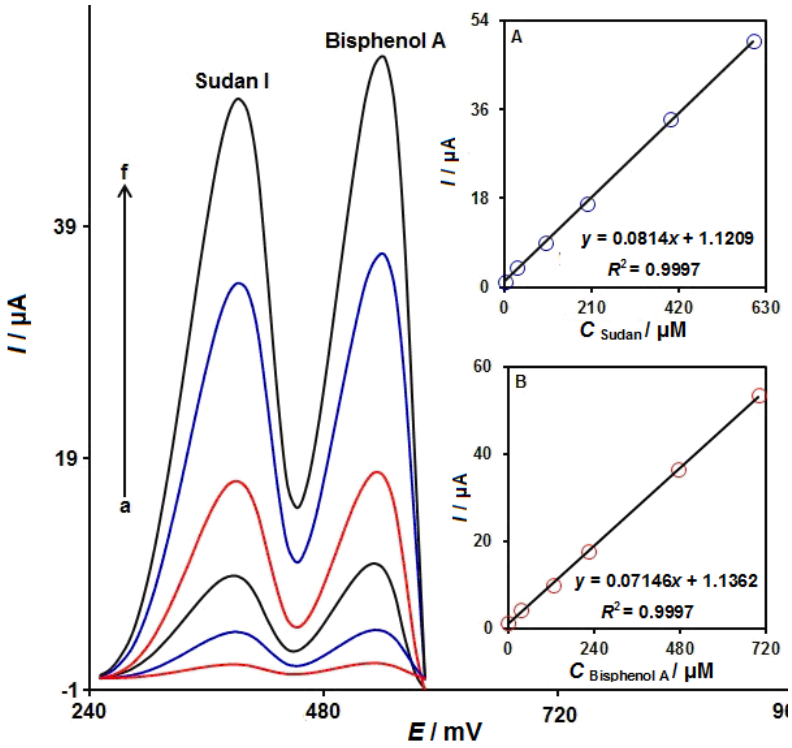

Figure 10. *DPVs of MWCNTs/Co3O4/SPGE in 0.1 M PBS, pH 7.0 containing different concentrations of Sudan I and Bisphenol A (a-f refer to mixed solutions of 0.5 + 0.5, 30.0 + 35.0, 100.0 + 125.0, 200.0 + 225.0, 400.0 + 475.0, and 600.0 + 700.0 µM of Sudan I and Bisphenol A, respectively). Inset A: plot of peak current as a function of Sudan I concentration. Inset B: plot of peak current as a function of Bisphenol A concentration*

Analysis of the real samples

To investigate the possibility of using MWCNTs/Co_3O_4/SPGE for the simultaneous detection of Sudan I and Bisphenol A in the real samples, electrochemical analysis were carried out in tomato paste, ketchup sauce, tap water and chili powder according to the standard addition approach. Table 1 reports the outputs and achieved recovery percentages of 97.6 to 103.6 % for these samples. These observed outputs suggest that MWCNTs/Co_3O_4/SPGE has acceptable practical viability for simultaneous detection of Sudan I and Bisphenol A.

***Table 1**. Determining of Sudan I and Bisphenol A in food samples (n = 5)*

Sample	Concentration spiked, µM		Concentration found, µM		Recovery,%		RSD, %	
	Sudan I	Bisphenol A	Sudan I	Bisphenol A	Sudan I	Bisphenol A	Sudan I	Bisphenol A
Ketchup sauce	0	0	-	-	-	-	-	-
	5.0	5.5	4.9	5.7	98.0	103.6	2.3	3.5
	7.0	7.5	7.2	7.4	102.9	98.7	2.7	2.1
Tomato pste	0	0	-	1.3	-	-	2.7	-
	4.0	4.5	4.1	4.4	102.5	97.8	3.0	1.9
	6.0	6.5	5.9	6.6	98.3	101.5	2.2	3.5
Chilli powder	0	0	-	-	-	-	-	-
	6.0	6.5	5.9	6.7	98.3	103.1	2.4	2.1
	8.0	8.5	8.1	8.3	101.2	97.6	2.8	1.6

Conclusion

In this work, MWCNTs/Co_3O_4 nanocomposite modified SPGE was prepared and introduced to simultaneously detect Sudan I and Bisphenol A. This modified electrode exhibited good electrocatalytic activity for the oxidation of Sudan I in 0.1 M PBS, pH 7.0 solution. The MWCNTs/Co_3O_4/SPGE linearly responded to Sudan I in the range from 0.05 to 600.0 µM with the LOD of 0.02 µM. Also, the application of MWCNTs/Co_3O_4 modified SPGE to simultaneously determine Sudan I and Bisphenol A was investigated. According to the results, two well-separated oxidation signals of Sudan I and Bisphenol A were obtained. Finally, the developed sensor system showed considerable potency for detection of Sudan I and Bisphenol A in some real samples including tomato paste, ketchup sauce, chili powder, and tap water.

References

[1] J. Li, H. Feng, J. Li, Y. Feng, Y. Zhang, J.Jiang, D. Qian, *Electrochimica Acta* **167** (2015) 226-236. https://doi.org/10.1016/j.electacta.2015.03.201
[2] X. Li, X. Sun, A. Zhou, Z. Zhu, M. Li, *New Journal of Chemistry* **45** (2021) 13585-13591. https://doi.org/10.1039/D1NJ02730A
[3] M. Stiborová, V. Martínek, H. Rýdlová, P. Hodek, E. Frei, *Cancer Research* **62** (2020) 5678-5684.
[4] N. B. Messaoud, M. E. Ghica, C. Dridi, M. B. Ali, C. M. Brett, *Sensors and Actuators B: Chemical* **253** (2017) 513-522. https://doi.org/10.1016/j.snb.2017.06.160
[5] N. B. Messaoud, A. A. Lahcen, C. Dridi, A. Amine, *Sensors and Actuators B: Chemical* **276** (2018) 304-312. https://doi.org/10.1016/j.snb.2018.08.092
[6] D. Jemmeli, E. Marcoccio, D. Moscone, C. Dridi, F. Arduini, *Talanta* **216** (2020) 120924. https://doi.org/10.1016/j.talanta.2020.120924
[7] E. J. Hoekstra, C. Simoneau, *Critical Reviews in Food Science and Nutrition* **53** (2013) 386-402. https://doi.org/10.1080/10408398.2010.536919

[8] A. Schecter, N. Malik, D. Haffner, S. Smith, T. R. Harris, O. Paepke, L. Birnbaum, *Environmental Science & Technology* **44** (2010) 9425-9430. https://doi.org/10.1021/es102785d
[9] J. Im, F. E. Löffler, *Environmental Science & Technology* **50** (2016) 8403-8416. https://doi.org/10.1021/acs.est.6b00877
[10] C. Sánchez-Brunete, E. Miguel, J. L. Tadeo, *Journal of Chromatography A* **1216** (2009) 5497-5503. https://doi.org/10.1016/j.chroma.2009.05.065
[11] E. Ertaş, H. Özer, C. Alasalvar, *Food Chemistry 105* (2007) 756-760. https://doi.org/10.1016/j.foodchem.2007.01.010
[12] A. S. Alnaimat, M. C. Barciela-Alonso, P. Bermejo-Barrera, *Microchemical Journal* **147** (2019) 598-604. https://doi.org/10.1016/j.microc.2019.03.026
[13] X. Wang, H. Zeng, Y. Wei, J. M. Lin, *Sensors and Actuators B: Chemical* **114** (2006) 565-572. https://doi.org/10.1016/j.snb.2005.06.020
[14] E. Mejia, Y. Ding, M. F. Mora, C. D. Garcia, *Food Chemistry* **102** (2007) 1027-1033. https://doi.org/10.1016/j.foodchem.2006.06.038
[15] M. I. López, I. Ruisánchez, M. P. Callao, *Spectrochimica Acta Part A: Molecular and Biomolecular Spectroscopy 111* (2013) 237-241. https://doi.org/10.1016/j.saa.2013.04.031
[16] Y. Zhang, Z. Zhang, Y. Sun, *Journal of chromatography A* **1129** (2006) 34-40. https://doi.org/10.1016/j.chroma.2006.06.028
[17] S. Wang, X. Wei, L. Du, H. Zhuang, *Luminescence* **20** (2005) 46-50. https://doi.org/10.1002/bio.804
[18] M. Pirozmand, A. Nezhadali, M. Payehghadr, L. Saghatforoush, *Eurasian Chemical Communications* **2** (2020) 1021-1032. https://doi.org/10.22034/ECC.2020.241560.1063
[19] A. Khodadadi, E. Faghih-Mirzaei, H. Karimi-Maleh, A. Abbaspourrad, S. Agarwal, V. K. Gupta, *Sensors and Actuators B: Chemical* **284** (2019) 568-574. https://doi.org/10.1016/j.snb.2018.12.164
[20] E. Burcu Aydın, *International Journal of Environmental Analytical Chemistry* **100** (2020) 363-377. https://doi.org/10.1080/03067319.2019.1679807
[21] S. Tajik, H. Beitollahi, F. G. Nejad, I. Sheikhshoaie, A. S. Nugraha, H. W. Jang, M. Shokouhimehr, *Journal of Materials Chemistry A* **9** (2021) 8195-8220. https://doi.org/10.1039/D0TA08344E
[22] W. H. Elobeid, A. A. Elbashir, *Progress in Chemical and Biochemical Research* **2** (2019) 24-33. https://doi.org/ 10.33945/SAMI/PCBR.2019.2.2433
[23] S. Jebril, L. Cubillana-Aguilera, J. M. Palacios-Santander, C. Dridi, *Materials Science and Engineering: B* **264** (2021) 114951. https://doi.org/10.1016/j.mseb.2020.114951
[24] H. Karimi-Maleh, K. Cellat, K. Arıkan, A. Savk, F. Karimi, F. Şen, *Materials Chemistry and Physics* **250** (2020) 123042. https://doi.org/10.1016/j.matchemphys.2020.123042
[25] S. Z. Bas, N. Yuncu, K. Atacan, M. Ozmen, *Electrochimica Acta* **386** (2021) 138519. https://doi.org/10.1016/j.electacta.2021.138519
[26] S. Tajik, H. Beitollahi, H. W. Jang, M. Shokouhimehr, *Talanta* **232** (2021) 122379. https://doi.org/10.1016/j.talanta.2021.122379
[27] L. Yang, S. Wang, L. Zhang, *International Journal of Electrochemical Science* **15** (2020) 11168-11179. https://doi.org/10.20964/2020.11.77
[28] F. Mehri-Talarposhti, A. Ghorbani-Hasan Saraei, L. Golestan, S. A. Shahidi, *Asian Journal of Nanosciences and Materials* **3** (2020) 313-320. https://doi.org/10.26655/AJNANOMAT.2020.4.5
[29] H. Karimi-Maleh, M. L. Yola, N. Atar, Y. Orooji, F. Karimi, P. S. Kumar, M. Baghayeri, *Journal of Colloid and Interface Science* **592** (2021) 174-185. https://doi.org/10.1016/j.jcis.2021.02.066

[30] M. A. Tapia, C. Perez-Rafols, R. Gusmao, N. Serrano, Z. Sofer, J. M. Díaz-Cruz, *Electrochimica Acta* **362** (2020) 137144. https://doi.org/10.1016/j.electacta.2020.137144
[31] A. Smart, A. Crew, R. Pemberton, G. Hughes, O. Doran, J. P. Hart, *TrAC Trends in Analytical Chemistry* **127** (2020) 115898. https://doi.org/10.1016/j.trac.2020.115898
[32] A. Vasilescu, G. Nunes, A. Hayat, U. Latif, J. L. Marty, *Sensors* **16** (2016) 1863. https://doi.org/10.3390/s16111863
[33] J. M. Díaz-Cruz, N. Serrano, C. Pérez-Ràfols, C. Ariño, M. Esteban, *Journal of Solid State Electrochemistry* **24** (2020) 2653-2661. https://doi.org/10.1007/s10008-020-04733-9
[34] F. G. Nejad, S. Tajik, H. Beitollahi, I. Sheikhshoaie, *Talanta* **228** (2021) 122075. https://doi.org/10.1016/j.talanta.2020.122075
[35] R. Abdi, A. Ghorbani-HasanSaraei, S. Naghizadeh Raeisi, F. Karimi, *Journal of Medicinal and Chemical Sciences* **3** (2020) 338-344. https://doi.org/ 10.26655/JMCHEMSCI.2020.4.3
[36] H. Houcini, F. Laghrib, M. Bakasse, S. Lahrich, M. A. El Mhammedi, *International Journal of Environmental Analytical Chemistry* **100** (2020) 1566-1577. https://doi.org/10.1080/03067319.2019.1655558
[37] H. Karimi-Maleh, F. Karimi, S. Malekmohammadi, N. Zakariae, R. Esmaeili, S. Rostamnia, V. K. Gupta, *Journal of Molecular Liquids* **310** (2020) 113185. https://doi.org/10.1016/j.molliq.2020.113185
[38] D. P. Rocha, A. L. Squissato, S. M. da Silva, E. M. Richter, R. A. Munoz, *Electrochimica Acta* **335** (2020) 135688. https://doi.org/10.1016/j.electacta.2020.135688
[39] M. Shahsavari, S. Tajik, I. Sheikhshoaie, F. G. Nejad, H. Beitollahi, *Microchemical Journal* **170** (2021) 106637. https://doi.org/10.1016/j.microc.2021.106637
[40] P. Prasad, N. Y. Sreedhar, *Chemical Methodologies* **2** (2018) 277-290. https://doi.org/10.22034/CHEMM.2018.63835
[41] H F. asanpour, M. Taei, M. Fouladgar, M. Salehi, *Quarterly Journal of Iranian Chemical Communication* **8** (2020) 135-144. https://doi.org/10.30473/ICC.2020.48000.1594
[42] Y. Wang, R. Zhou, C. Wang, G. Zhou, C. Hua, Y. Cao, Z. Song, *Journal of Alloys and Compounds* **817** (2020) 153286. https://doi.org/10.1016/j.jallcom.2019.153286
[43] S. S. Mahmood, A. J. Atiya, F. H. Abdulrazzak, A. F. Alkaim, F. H. Hussein, *Journal of Medicinal and Chemical Sciences* **4** (2021) 225-229. https://doi.org/10.26655/JMCHEMSCI.2021.3.2
[44] E. Shojaei, M. Masrournia, A. Beyramabadi, H. Behmadi, *Eurasian Chemical Communications* **2** (2020) 750-759. https://doi.org/10.33945/SAMI/ECC.2020.7.2
[45] H. Karimi-Maleh, F. Karimi, Y. Orooji, G. Mansouri, A. Razmjou, A. Aygun, F. Sen, *Scientific Reports* **10** (2020) 1-13. https://doi.org/10.1038/s41598-020-68663-2
[46] F. Laghrib, N. Ajermoun, M. Bakasse, S. Lahrich, M. A. El Mhammedi, *International Journal of Environmental Analytical Chemistry* **100** (2020) 1309-1324. https://doi.org/10.1080/03067319.2019.1651851
[47] J. Ghodsi, A. A. Rafati, Y. Shoja, *Advanced Journal of Chemistry-Section A* **1** (2018) 39-55. https://doi.org/10.29088/SAMI/AJCA.2018.5.3955
[48] H. Beitollahi, S. Tajik, F. G. Nejad, M. Safaei, *Journal of Materials Chemistry B* **8** (2020) 5826-5844. https://doi.org/10.1039/D0TB00569J
[49] M. S. Sengar, S. Saxena, S. P. Satsangee, R. Jain, *Journal of Applied Organometallic Chemistry* **1** (2021) 95-108. https://doi.org/10.22034/JAOC.2021.289344.1023
[50] C. Chen, R. Ran, Z. Yang, R. Lv, W. Shen, F. Kang, Z. H. Huang, *Sensors and Actuators B: Chemical* **256** (2018) 63-70. https://doi.org/10.1016/j.snb.2017.10.067
[51] J. R. Maluta, T. C. Canevari, S. A. Machado, *Journal of Solid State Electrochemistry* **18** (2014) 2497-2504. https://doi.org/10.1007/s10008-014-2505-0
[52] M. I. Sabela, T. Mpanza, S. Kanchi, D. Sharma, K. Bisetty, *Biosensors and Bioelectronics* **83** (2016) 45-53. https://doi.org/10.1016/j.bios.2016.04.037

[53] A. E. Vilian, B. Dinesh, M. Rethinasabapathy, S. K. Hwang, C. S. Jin, Y. S. Huh, Y. K. Han, *Journal of Materials Chemistry A* **6** (2018) 14367-14379. https://doi.org/10.1016/j.bios.2016.04.037
[54] S. Buratti, B. Brunetti, S. Mannino, *Talanta* **76** (2008) 454-457. https://doi.org/10.1016/j.talanta.2008.03.031
[55] Y. Xia, H. Dai, H. Jiang, L. Zhang, *Catalysis Communications* **11** (2010) 1171-1175. https://doi.org/10.1016/j.catcom.2010.07.005
[56] N. R. Radwan, M. S. El-Shall, H. M. Hassan, *Applied Catalysis A: General* **331** (2007) 8-18. https://doi.org/10.1016/j.apcata.2007.07.005